

# Recrystallization as a Growth Mechanism for Whiskers on Plastically Deformed Sn Films

JAEWON CHANG,<sup>1</sup> SUNG K. KANG,<sup>2</sup> JAE-HO LEE,<sup>3</sup> KEUN-SOO KIM,<sup>4</sup>  
and HYUCK MO LEE<sup>1,5</sup>

1.—Department of Materials Science and Engineering, KAIST, 291 Daehak-ro, Yuseong-gu, Daejeon 305-701, Republic of Korea. 2.—IBM T.J. Watson Research Center, Yorktown Heights, NY 10598, USA. 3.—Department of Materials Science and Engineering, Hongik University, 72-1 Sangsu-dong, Mapo-gu, Seoul 121-791, Republic of Korea. 4.—Department of Display Engineering, Hoseo University, Asan 336-795, Republic of Korea. 5.—e-mail: hmlee@kaist.ac.kr

Sn whiskers are becoming a serious reliability issue in Pb-free electronic packaging applications. Sn whiskers are also observed in connector parts of electronics as well as on electroplated surface finishes. Sn whiskers found in connector parts are known to behave differently from the typical Sn whiskers reported on electroplated Sn surfaces. In this study, Sn whiskers on plastically deformed Sn-rich films were investigated to understand their growth behavior to establish mitigation strategies for Sn-rich films used in connectors. Therefore, a microhardness indentation technique was applied to plastically deform electroplated matte Sn samples, followed by temperature/humidity (T/H) testing (30°C, dry air). Each sample was examined by scanning electron microscopy at regular time intervals up to 4000 h. Various morphologies of Sn whiskers on plastically deformed matte Sn films were observed, and their growth statistics and kinetics are analyzed in terms of the plating conditions and plastic deformation by using transmission electron microscopy, x-ray diffraction, and the focused ion-beam technique. Sn whiskers were observed on plastically deformed regions of thin (2- $\mu\text{m}$ ) and thick (10- $\mu\text{m}$ ) matte Sn films, regardless of the current density applied. Plastic deformation was found to promote whisker formation on matte Sn films. A high density of dislocations and newly formed fine Sn subgrains were observed in deformed grains. In addition, the recrystallized grains and  $\text{Cu}_6\text{Sn}_5$  intermetallic compound grew further with increasing time. Finally, a growth mechanism for deformation-induced Sn whiskers is proposed based on a recrystallization model combined with the formation of  $\text{Cu}_6\text{Sn}_5$ .

**Key words:** Sn whiskers, plastic deformation, external pressure, recrystallization

## INTRODUCTION

A Sn whisker is an electrically conductive single- (or poly)crystalline structure that is spontaneously formed on a Sn-rich surface. Sn whiskers are commonly found on electroplated Sn surfaces used in electronic packaging. Sn whiskers are also found in connector parts of electronics, for example, flexible

printed circuits<sup>1</sup> and universal serial buses (USBs).<sup>2</sup> The behaviors of Sn whiskers in connector parts are expected to be different from the typical Sn whiskers found on electroplated Sn surfaces. Sn whisker growth in connector parts is accelerated by the external pressure induced by repetitive motions of plugging and unplugging. Sn whiskers that are induced by external pressure can cause serious reliability issues in electronics, such as electronic short circuits and debris/contamination similar to typical Sn whiskers on electroplated Sn surfaces.

(Received July 24, 2014; accepted June 23, 2015;  
published online July 8, 2015)

Such problems could be resolved through a reflow process<sup>3</sup> or alloying with lead (Pb),<sup>4</sup> thereby suppressing formation and growth of Sn whiskers. However, use of Pb is restricted legally due to its harmful health effects and environmental concerns according to the European Union restriction of hazardous substances legislation.<sup>5</sup>

A limited number of studies have been reported on pressure-induced Sn whiskers compared with the typical Sn whiskers on electroplated surface finishes.<sup>6,7</sup> Also, not many growth mechanisms or mitigation strategies for pressure-induced Sn whiskers have been discussed in the literature. Nevertheless, some models have been proposed to explain the formation and growth of pressure-induced Sn whiskers. Moriuchi et al.<sup>8</sup> reported that the growth mechanism for pressure-induced Sn whiskers involves a crystallographic change: the  $\beta$ -Sn structure transforms into a cubic  $\alpha$ -Sn structure due to the external pressure. In addition, internal stress occurs between the original  $\beta$ -Sn and the deformed  $\alpha$ -Sn. Thus, whiskers with  $\beta$ -Sn structure are generated via relaxation of this internal stress. Shibutani et al.<sup>1</sup> described a growth mechanism for pressure-induced Sn whiskers with creep behavior. When an external pressure is applied to a Sn surface, the material below the pressed area expands in the orthogonal directions due to the deformation. Because the melting point of Sn is relatively low, the plated Sn surface creeps, even at room temperature. This creep induces multiaxial stress concentration outside the compressed area. Although stress relaxation occurs, multiaxial stress components remain as residual stresses, acting on grain boundaries in the plated Sn layer. These stresses can cause stress-induced atomic migration and the formation of whiskers.

The above-mentioned growth mechanisms for pressure-induced Sn whiskers have been proposed for situations with static pressure and very long holding time. However, the plastic deformation induced by an initial external pressure is more important than that induced by a static pressure in the case of connectors, which are subjected to repetitive external pressures. Thus, in this study, matte Sn films were plastically deformed with a large external pressure for a short time to provide a loading situation similar to that in connector parts. The resulting whiskers are defined as deformation-induced Sn whiskers in this paper. The effects of plastic deformation on Sn whisker growth are investigated and compared with our previous work reporting the behavior of Sn whisker growth on nondeformed electroplated Sn films.<sup>9</sup> In addition, the density, length, and kinetics of the Sn whiskers on plastically deformed regions were investigated for various plating thicknesses and electroplating current densities to examine the effects of these variables on the mitigation of deformation-induced Sn whiskers. The microstructures of Sn whiskers and deformed Sn films were also evaluated. Finally,

a growth mechanism for deformation-induced Sn whiskers is proposed.

## EXPERIMENTAL PROCEDURES

Commercially available matte Sn low-whisker formulations were used for electroplating. The Sn films were electroplated using a direct-current power supply with a dimensionally stable anode in a small-scale bath with capacity of 250 mL. As a substrate, TiW(0.16  $\mu\text{m}$ )/Ni(2.4  $\mu\text{m}$ )/Cu(0.8  $\mu\text{m}$ ) metallization was deposited by chemical vapor deposition onto a 750- $\mu\text{m}$  Si wafer. The Sn films were electroplated at current densities of 10  $\text{mA}/\text{cm}^2$  and 25  $\text{mA}/\text{cm}^2$  at plating temperature of 40°C to yield two different plating thicknesses: 2  $\mu\text{m}$  (thin) and 10  $\mu\text{m}$  (thick).

After electroplating, the Sn films were plastically deformed using a microhardness tester equipped with a 136° angle Vickers diamond square indenter (microhardness tester, CM-100; Clark). The same external load of 100 gf was used regardless of the plating thickness. After only 5 s, the external load was removed from the Sn films. The deformation speed was 50  $\mu\text{m}/\text{s}$ . Figure 1 shows a schematic of the external loading process. The external pressure, calculated as the load per unit area, was 1387 MPa and 255 MPa in the thin and thick Sn film, respectively. These external pressure values are much larger than the yield stress of Sn, which is 9 MPa to 14 MPa.<sup>10</sup>

Each group of samples was stored under ambient (30°C, dry air) condition as per the JESD201A standard of the Joint Electron Device Engineering Council (JEDEC).<sup>11</sup> The surface morphologies of the plastically deformed regions of Sn films were examined every 200 h up to 1000 h, then every 1000 h until 4000 h using a scanning electron microscope (SEM, XL30; Philips). The plastically deformed regions of Sn films were then sectioned using a focused-ion beam (FIB, Quanta 3D FEG; FEI Co., and Helios Nanolab 450 F1; FEI Co.) system, and the microstructures of the sectioned sides were examined using FIB ion-channeling imaging. In addition, a particular whisker was sectioned by the FIB system and then analyzed using transmission electron microscopy (TEM, Tecnai G2 F30; FEI Co.) and

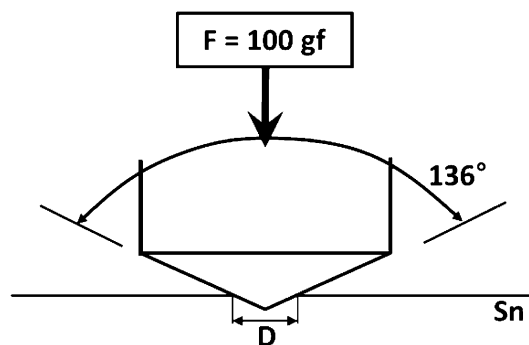


Fig. 1. Schematic diagram of external loading in this study.

energy-dispersive x-ray spectroscopy (EDAX) to examine the microstructure, intermetallic compound (IMC) formation, and other features.

## RESULTS AND DISCUSSION

### As-Deformed Sn Films

The surface morphologies were investigated as soon as the external pressure was removed. Figure 2 presents the surface morphologies around a deformed region on a Sn film right after the external pressure was applied. The matte Sn was deformed immediately after electroplating. The surfaces of the Sn films were severely deformed for both the thin and thick Sn films. Although the Vickers hardness indenter has a diamond shape, the plastically deformed regions showed a roughly circular shape, and the deformed regions were in close contact with the indenter because Sn is a very soft metal and the applied external pressure was large. The diameters of the plastically deformed regions were approximately  $30\ \mu\text{m}$  and  $70\ \mu\text{m}$  for the thin and thick Sn films, respectively. The diameters of the plastically deformed regions were different from

each other because of the different plating thicknesses, even though the same external load was applied. Sn whiskers were not observed around or in the plastically deformed regions right after the external pressure was applied. The plastically deformed regions of the Sn films were also investigated using a FIB incision for their microstructures in cross-sections directly after deformation. Figure 3 presents ion-channeling images of the plastically deformed regions of the thin and thick Sn films. Platinum (Pt) was coated on the surfaces of the deformed regions to reduce the damage induced by the FIB incision process. For both the thin and thick Sn films, the cross-section microstructures were severely deformed by the external pressure as well as the surface morphologies. The Sn film was pushed away from the center of the deformed region, and the plating thickness increased toward the edge of the deformed region. According to our previous work, thin matte Sn consists of columnar grains whereas thick matte Sn (plated with the low-whisker formulation used in this study) consists of both columnar and equiaxed grains.<sup>9</sup> However, the microstructures of the deformed regions changed to

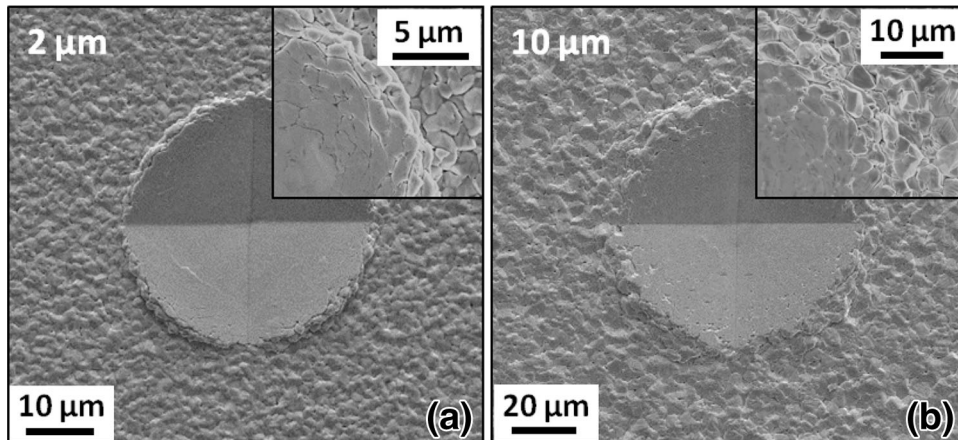


Fig. 2. SEM images of as-deformed region for matte Sn surfaces: (a) thin films electroplated at current density of  $25\ \text{mA}/\text{cm}^2$ , and (b) thick films electroplated at current density of  $25\ \text{mA}/\text{cm}^2$ .

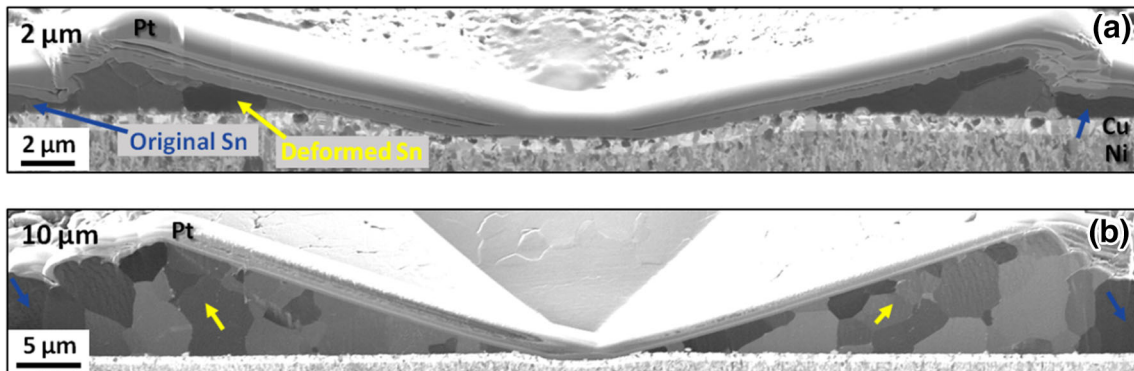


Fig. 3. Ion-channeling images of cross-sectioned as-deformed matte Sn surfaces: (a) thin films electroplated at current density of  $25\ \text{mA}/\text{cm}^2$ , and (b) thick films electroplated at current density of  $25\ \text{mA}/\text{cm}^2$ .

small columnar grains in the thin matte Sn, and to large inclined columnar and equiaxed grain structures in the thick matte Sn. The original grain structures remained unchanged outside of the deformed region.  $\text{Cu}_6\text{Sn}_5$  and  $\text{Cu}_3\text{Sn}$  IMCs were not observed at the interface between the Sn film and Cu substrate layer for either the thin or thick Sn films.

### Effect of Plastic Deformation on Whisker Growth in Sn Films

The surfaces of the plastically deformed regions of Sn films stored under ambient condition after 4000 h were investigated. All deformed Sn films after 4000 h contained Sn whiskers on the plastically deformed regions, regardless of the plating thickness or current density, as indicated in Fig. 4. Sn whiskers were observed only on the edge of the deformed regions for the thin Sn films, whereas Sn whiskers were observed both on the edge and inside the deformed regions for the thick Sn films. The Sn whiskers were classified into three types according to their shape and morphology: filament, nodule, and mixed whiskers, as illustrated in Fig. 5. Filament-type whiskers grow with a constant diameter from their base to the tip; curved and kinked whiskers were also included as filament-type whiskers if their diameter was maintained during

growth. However, the diameter of nodule-type whiskers is not maintained during growth. Filament-type whiskers were mostly observed at the edge of deformed regions, whereas nodules were observed both at the edge and inside of deformed regions. Finally, if a filament-type whisker was present on a nodule, it was defined as a mixed whisker. Mixed whiskers have been reported in previous works. Sarobol et al.<sup>12</sup> reported whisker-top hillocks, which have a whisker top due to initial grain-boundary pinning and a subsequent hillock that grows due to grain-boundary migration. In addition, Boettinger et al.<sup>7</sup> reported filament-type whiskers grown on a hillock base that grew first. Both whiskers were observed on electroplated Sn-Cu surfaces.

The total number of Sn whiskers including filament, nodule, and mixed whiskers was counted in the deformed regions as well as the surrounding area to evaluate the propensity for deformation-induced Sn whiskers. The boundary for counting Sn whiskers was twice the diameter of the deformed region from the center. Figure 6 indicates the total number of Sn whiskers on the deformed regions of the thin and thick Sn films (electroplated at current densities of  $10 \text{ mA/cm}^2$  and  $25 \text{ mA/cm}^2$ ), stored under ambient condition for 4000 h. The total numbers of Sn whiskers on the deformed regions of

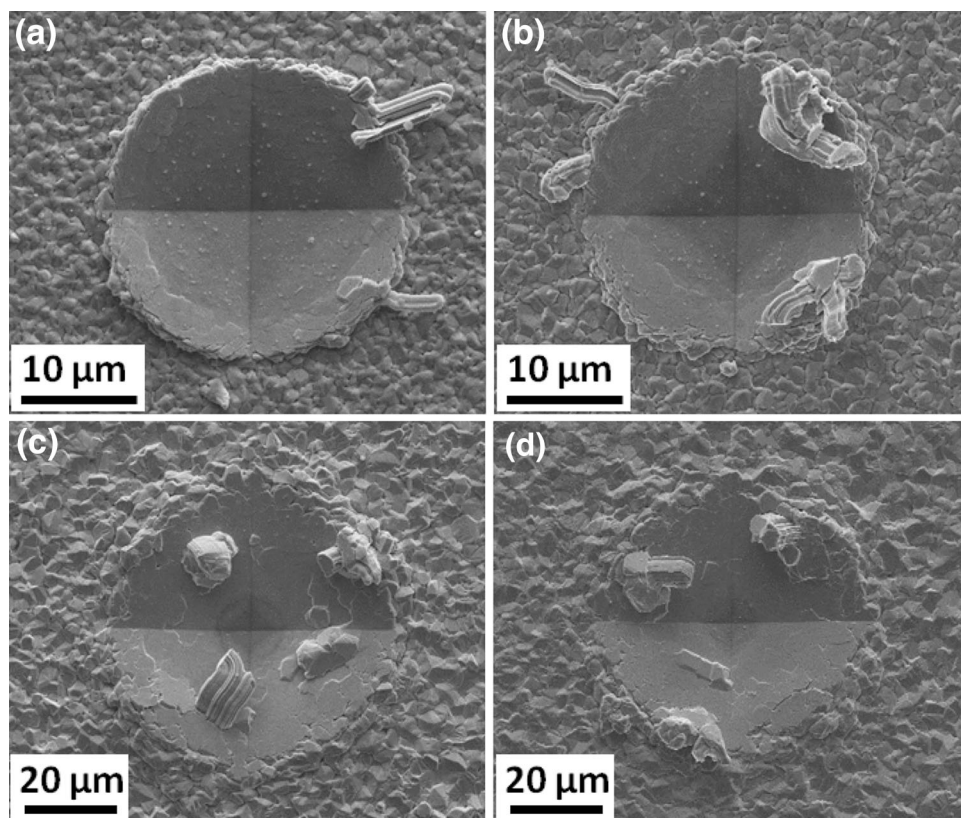


Fig. 4. SEM images of plastically deformed regions for matte Sn stored at  $30^\circ\text{C}$  in dry air after 4000 h: (a, b) thin and (c, d) thick films; electroplated at current density of (a, c)  $10 \text{ mA/cm}^2$  and (b, d)  $25 \text{ mA/cm}^2$ .

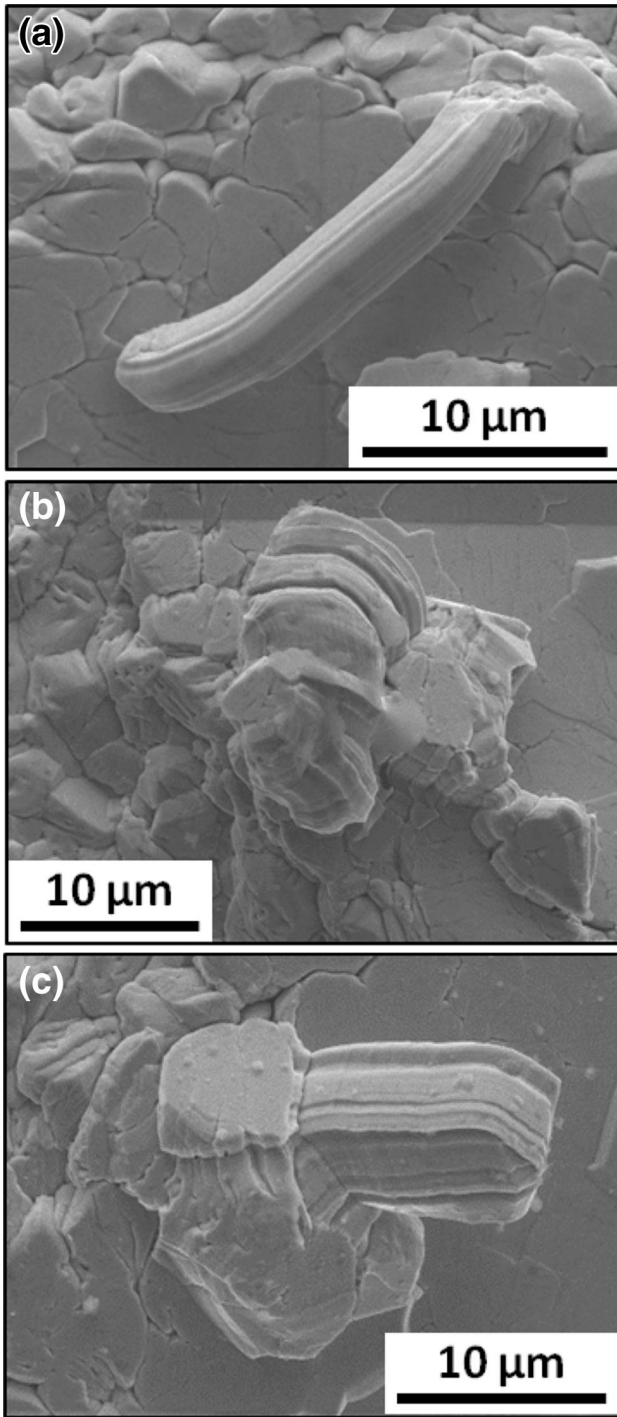


Fig. 5. Different types of Sn whiskers on plastically deformed region of matte Sn in this study: (a) filament, (b) nodule, and (c) mixed whisker.

Sn films were 4.50, 6.42, 4.25, and 4.40 for plating thickness (current density) of  $2\ \mu\text{m}$  ( $10\ \text{mA}/\text{cm}^2$ ),  $2\ \mu\text{m}$  ( $25\ \text{mA}/\text{cm}^2$ ),  $10\ \mu\text{m}$  ( $10\ \text{mA}/\text{cm}^2$ ), and  $10\ \mu\text{m}$  ( $25\ \text{mA}/\text{cm}^2$ ), respectively. The thin Sn films electroplated at  $25\ \text{mA}/\text{cm}^2$  had the largest Sn whisker density, which is consistent with the results from the nondeformed matte Sn.<sup>9</sup>

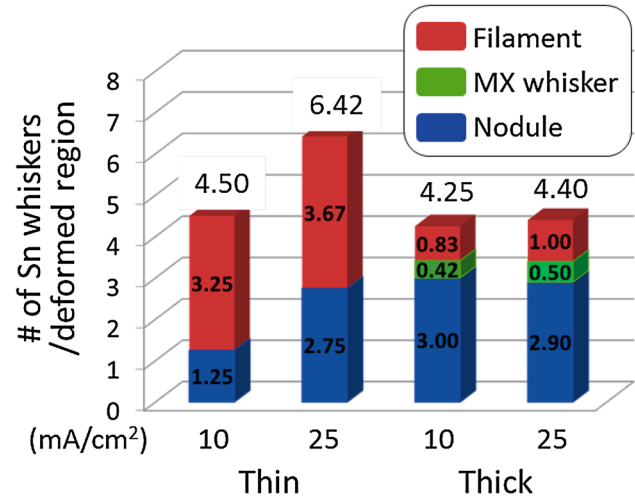


Fig. 6. Sn whisker density of plastically deformed regions of matte Sn using  $10\ \text{mA}/\text{cm}^2$  and  $25\ \text{mA}/\text{cm}^2$  current densities for samples with different plating thicknesses stored at  $30^\circ\text{C}$  in dry air after 4000 h.

According to the JEDEC standard,<sup>11</sup> the number of whiskers was converted from per deformed region to per  $\text{mm}^2$  area to evaluate the effect of plastic deformation on the density of Sn whiskers, as summarized in Table I. The total number of Sn whiskers per  $\text{mm}^2$  area was 1591, 2270, 276, and 285 for plating thickness (current density) of  $2\ \mu\text{m}$  ( $10\ \text{mA}/\text{cm}^2$ ),  $2\ \mu\text{m}$  ( $25\ \text{mA}/\text{cm}^2$ ),  $10\ \mu\text{m}$  ( $10\ \text{mA}/\text{cm}^2$ ), and  $10\ \mu\text{m}$  ( $25\ \text{mA}/\text{cm}^2$ ), respectively. The densities of the Sn whiskers in the deformed regions were much larger than those in the nondeformed matte Sn studied in previous work.<sup>9</sup> This finding indicates that plastic deformation induced by external pressure promotes whisker formation on Sn films. Filament-type whiskers, which are more critical to reliability, were the commonest whisker type observed for the thin Sn films. However, for the thicker plating thickness, the number of filament-type whiskers decreased and nodules dominated on thick Sn films, regardless of the current density. The reason for this change is that the external pressure applied to the thin Sn films was much larger than that applied to the thick Sn films. Yang and Li<sup>13</sup> reported that smaller external stresses under a threshold tend to produce nodule-type whiskers, whereas larger external stresses over the threshold tend to produce long whiskers. This is because high local stresses can cause surface oxide cracking, which would increase the propensity to extrude the Sn grain itself from the Sn surface. In addition, mixed whiskers were only observed on thick Sn films. The effect of the current density on the number of Sn whiskers in deformed regions was also investigated. When the current density was increased, the number of whiskers increased for the thin Sn films, whereas the thick Sn films had a similar number of whiskers regardless of the current density. This result can be understood based on

**Table I. Sn whisker density and length on plastically deformed regions and nondeformed regions,<sup>9</sup> and grain diameter<sup>9</sup> for matte Sn using 10 mA/cm<sup>2</sup> and 25 mA/cm<sup>2</sup> current densities for samples with different plating thicknesses stored at 30°C in dry air after 4000 h**

Plastically Deformed Matte Sn	Plating Thickness			
	2 $\mu\text{m}$		10 $\mu\text{m}$	
	10 mA/cm <sup>2</sup>	25 mA/cm <sup>2</sup>	10 mA/cm <sup>2</sup>	25 mA/cm <sup>2</sup>
Total Number of Whiskers				
w/PD	1591	2270	276	285
w/o <sup>9</sup>	59	193	59	80
Length of whiskers ( $\mu\text{m}$ )	Avg.	Max.	Avg.	Max.
w/PD	5.6	8.3	18.2	25.4
w/o <sup>9</sup>	19.2	90.0	25.0	96.0
Grain diameter ( $\mu\text{m}$ ) <sup>9</sup>	1.5	2.0	4.8	4.5

the relationship between the grain size of the Sn film and the current density. The grain size of the thin Sn films increased with increasing current density, whereas no significant differences in grain size were observed for the thick Sn films with increasing current density, as indicated in Table I. As the grain size increased, the number of whiskers was prone to increase for the same plating thickness because the minimum load to produce whiskers tends to be lower for large grains.<sup>14</sup>

The length of Sn whiskers was also investigated as a function of plating thickness. Table I lists the average and maximum length of Sn whiskers on plastically deformed Sn films stored under ambient condition for 4000 h. The lengths of nodules are excluded because they do not grow long enough and it is difficult to objectively measure the length of nodules. The average length of Sn whiskers in the deformed regions was 5.6  $\mu\text{m}$  and 18.2  $\mu\text{m}$  for the thin and thick Sn film, respectively. The length of the longest whiskers was 25.4  $\mu\text{m}$ , which was observed for thick Sn films. The thick Sn films had longer Sn whiskers than the thin Sn films because thick Sn films are expected to need a longer time to completely eliminate the stress than thin Sn films. This result is consistent with previous work by our group indicating that thick Sn films had longer Sn whiskers than thin Sn films on nondeformed electroplated matte Sn surfaces.<sup>9</sup> However, the length of whiskers in the deformed region (approximately 25.4  $\mu\text{m}$ ) was much shorter than that of whiskers for the nondeformed Sn films (approximately 96  $\mu\text{m}$ ).

### Kinetics of Sn Whiskers on Plastically Deformed Sn Films

The plastically deformed regions were observed by SEM in a time series to investigate the formation and growth of Sn whiskers. Figure 7 presents a time series of SEM images showing the formation and growth of deformation-induced Sn whiskers for thin and thick Sn films for three types of whiskers. It is interesting to note that several cracks were observed on the surfaces before nodules formed. The

growth sequence of mixed whiskers was similar to the observation by Boettinger et al.<sup>7</sup> nodules grow first, then the filament grows on top.

The changes in the numbers of whiskers with time were evaluated using the time-series SEM images. Figure 8a plots the number of whiskers with time in terms of Sn film thickness (2  $\mu\text{m}$  versus 10  $\mu\text{m}$ ) and current density (10 mA/cm<sup>2</sup> versus 25 mA/cm<sup>2</sup>). For thin Sn films, the formation of whiskers started at 200 h and ended well before 400 h. However, for thick Sn films, the whiskers formed continuously after 400 h until 2000 h. This result indicates that the driving forces to form whiskers disappeared in a relatively short time for the thin Sn films, whereas the driving forces existed for a longer time for the thick Sn films. In addition, the plating current density had no effect on the changes in the number of whiskers with time. Further analysis on the changes in the number of whiskers with time was carried out in terms of the three types of whiskers—filament, nodule, and mixed whiskers—only for thick Sn films, as shown in Fig. 8b and c. It was difficult to observe the changes in whisker population in the thin Sn films because most whiskers had already formed before 200 h, which was the first observation time. Nodules nucleated more at early times than filament-type whiskers because the threshold energy to form nodules is expected to be lower than that to form filament-type whiskers. In addition, filament whiskers on mixed whiskers undergo changes similar to those of filament-type whiskers in deformed regions, which were mostly formed from 600 h to 800 h. The changes of whisker length with time were also investigated. Figure 9 depicts the change in length of filament-type whiskers with time for the thin and thick Sn films. As noted in Figs. 7 and 9, formation and growth of whiskers completed by 400 h on thin Sn films, whereas whiskers grew continuously until 2000 h on thick Sn films. The growth rates of whiskers, i.e., the change in length over the time, was estimated to be  $6.35 \times 10^{-10}$  cm/s and  $2.64 \times 10^{-10}$  cm/s for the thin and thick films, respectively. The growth rate

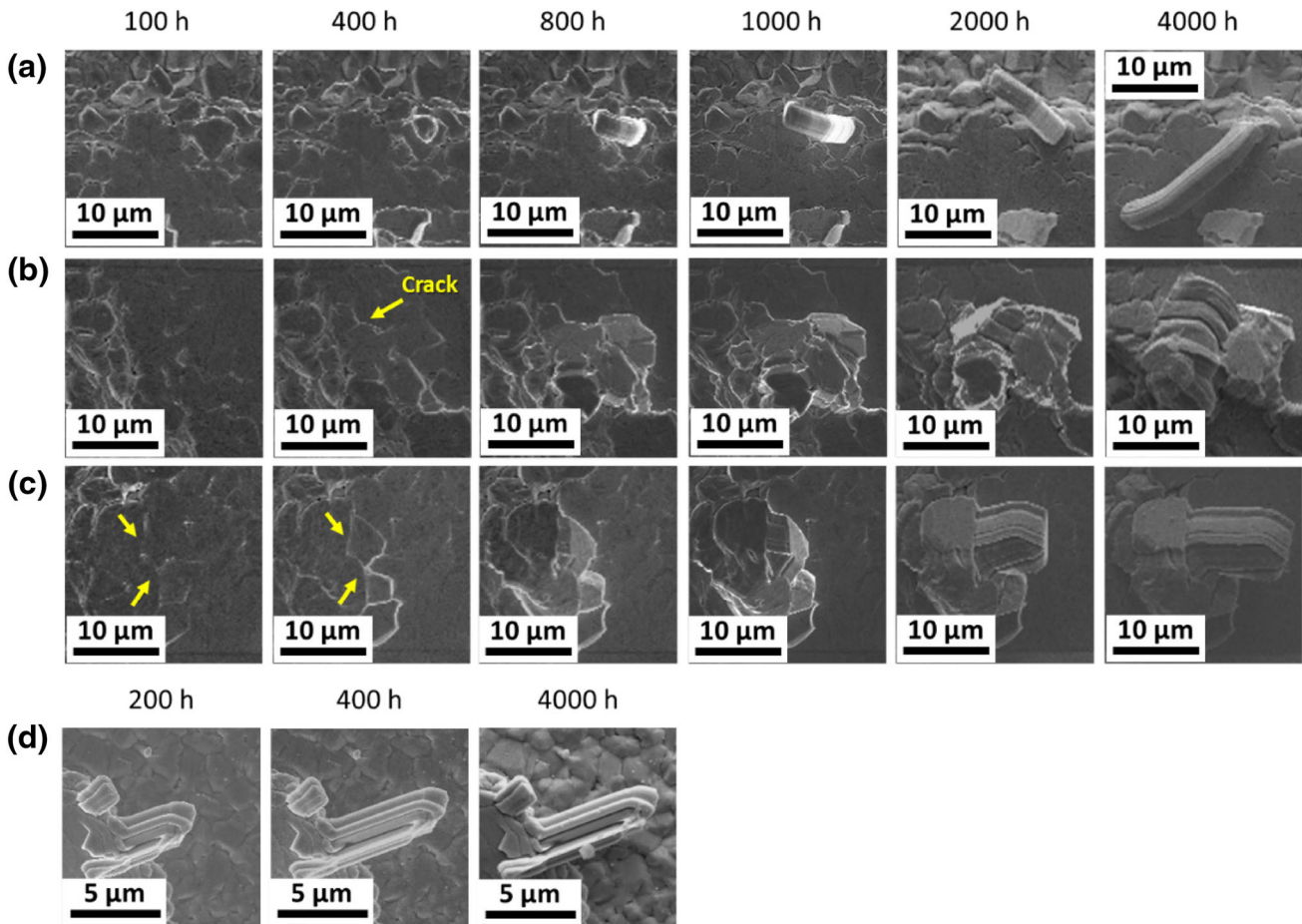


Fig. 7. Time-series SEM images showing formation and growth of deformation-induced Sn whiskers for thin and thick Sn films for three types of whiskers on matte Sn stored at 30°C in dry air after 4000 h: (a) filament, (b) nodule and (c) mixed whisker for thick Sn films, and (d) filament for thin Sn films.

of filament whiskers for 2- $\mu\text{m}$  film was found to be more than twice as fast as for 10- $\mu\text{m}$  film.

### Microstructure of Sn Whiskers on Plastically Deformed Sn Films

To understand the behavior of Sn whiskers in plastically deformed regions induced by an external pressure, the cross-section microstructures were examined by employing the FIB cross-section and ion-channeling image technique. The plastically deformed regions were FIB cross-sectioned from the center to the edge, including the root of a whisker and the adjacent grains, to observe the microstructure of both the whisker and the neighboring grains. Figure 10a shows a filament-type whisker stored under ambient condition for 500 h for thin Sn film. A filament-type whisker was observed at the junction between two grains. In addition, the grains in contact with the whisker became larger than the grains in the as-plated Sn film.<sup>9</sup> Figure 10b shows a nodule stored under ambient condition for 4000 h for thick Sn film. The nodule was uplifted through

the surface as a grain itself. The nodule and its neighboring grains became larger than the grains in the as-plated films,<sup>9</sup> similar to the grains in the thin Sn films.  $\text{Cu}_6\text{Sn}_5$  IMC was observed at the interface between the Sn film and Cu substrate layer for both the thin and thick Sn films. Filament-type whiskers were commonly observed in shallow grains, whereas nodules were more observed in deep grains. This observation is consistent with the results of previous work by Sarobol et al.<sup>12</sup>

To study the microstructures around the root of a whisker, cross-sectional TEM samples were prepared to closely observe the root of the whisker shown in Fig. 10a. A FIB was used to etch two rectangular holes into the finish separated by a thin wall of a whisker. The location of the two holes was selected to have a whisker on top of the wall between them. After etching, the thickness of the wall was less than 100 nm, such that it was transparent to 300-keV electrons. The thin wall contained a thin vertical section of the whisker, the root of the whisker, and several grains surrounding the whisker. Figure 11 shows bright-field (BF),

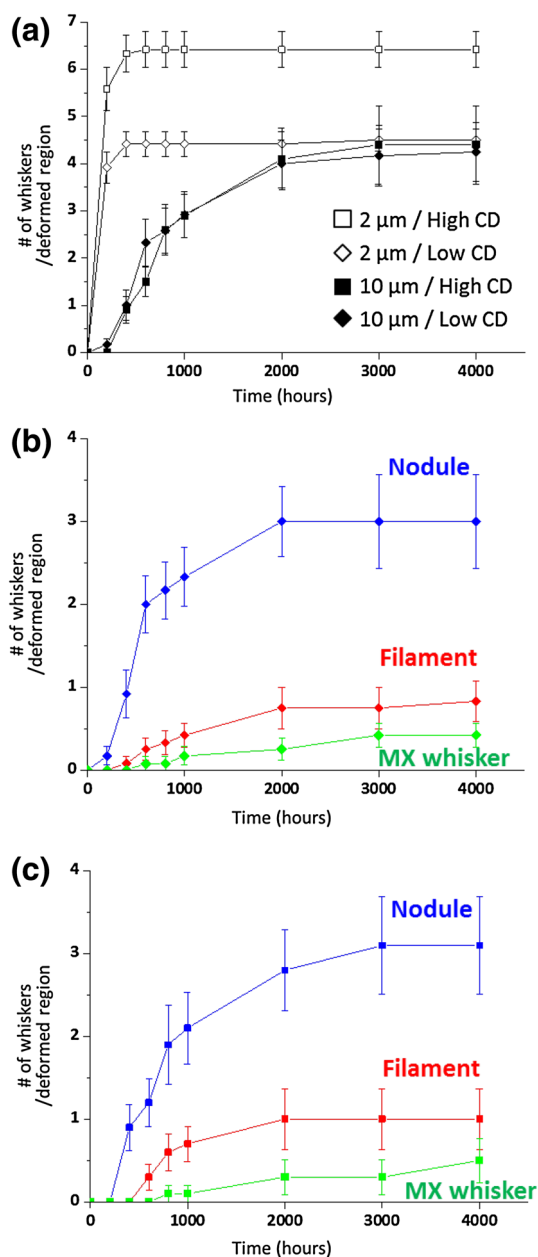


Fig. 8. Changes in the number of whiskers with time (a) for thin and thick Sn films electroplated with current densities of 10 mA/cm<sup>2</sup> and 25 mA/cm<sup>2</sup>, and for three types of whiskers for thick Sn films electroplated with current densities of (b) 10 mA/cm<sup>2</sup> and (c) 25 mA/cm<sup>2</sup>.

dark-field (DF), and high-resolution TEM (HRTEM) images, and selected-area electron diffraction (SAED) patterns of the grains and grain-boundary structures around the root of a filament-type whisker. There are highly accumulated dislocations in grain boundaries, caused by external pressures. Several defects, such as dislocations, and bending contours are observed in the filament-type whisker in Fig. 11b. Analysis of the SAED patterns in Fig. 11c indicated that the filament-type whisker had a body-centered tetragonal (BCT) single-crystalline

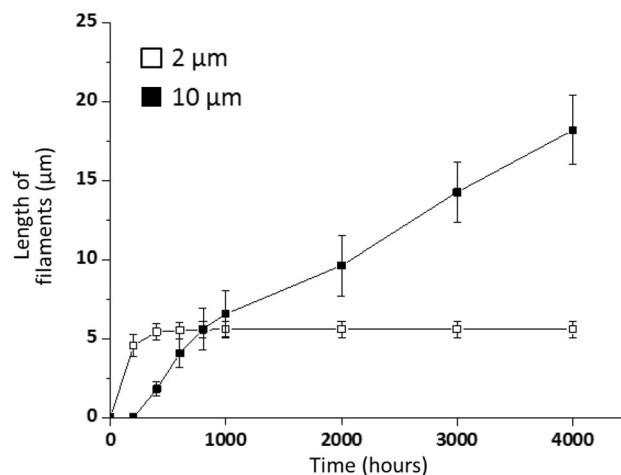


Fig. 9. Length change of filament-type whiskers with time for thin and thick Sn films.

structure with lattice parameters of  $a = 5.819 \text{ \AA}$  and  $c = 3.175 \text{ \AA}$ .<sup>15</sup> The growth direction of the filament-type whisker was  $[-111]$ . Figure 11d and e shows BF TEM images of the grains neighboring the filament-type whisker: one grain directly contacted by the external pressure and another grain under the filament-type whisker. Similar to the filament-type whisker, many defects were present in the grains, having a BCT single-crystalline rather than an  $\alpha$ -Sn crystalline structure, as shown in Fig. 11g. This suggests that phase transformations were not observed in this study, different from the work of Moriuchi et al.<sup>8</sup> In addition, very fine particles of 100 nm, different from dislocations, were observed inside the grains neighboring the filament-type whisker. The fine particles had a different grain orientation from the parent grain, based on analysis of the HRTEM images, as shown in Fig. 11f. In addition, the fine particles were identified as pure Sn by EDAX analysis. Based on SAED analysis in Fig. 11g, some patterns (marked by red arrows) were different from the parent grain patterns, indicating a growth direction of  $[-111]$ . These patterns matched with the fine particles in the DF images shown in Fig. 11h. Thus, the fine particles were identified as Sn subgrains.

To confirm the presence of fine Sn subgrains, the nodules and as-deformed Sn films were further analyzed by TEM. In as-deformed Sn films, Sn subgrains were only observed in grains that were directly contacted by an external pressure, as shown in Fig. 12, whereas there were no Sn subgrains in as-plated Sn films. This result implies that the Sn subgrains formed during the plastic deformation. In addition, Sn subgrains formed first at highly deformed grains, which contained highly accumulated dislocations. However, no newly formed Sn subgrains were observed in the nodule, as shown in Fig. 13, which presents BF TEM images and SAED patterns of a fully grown nodule stored under ambient condition for 4000 h. There were no



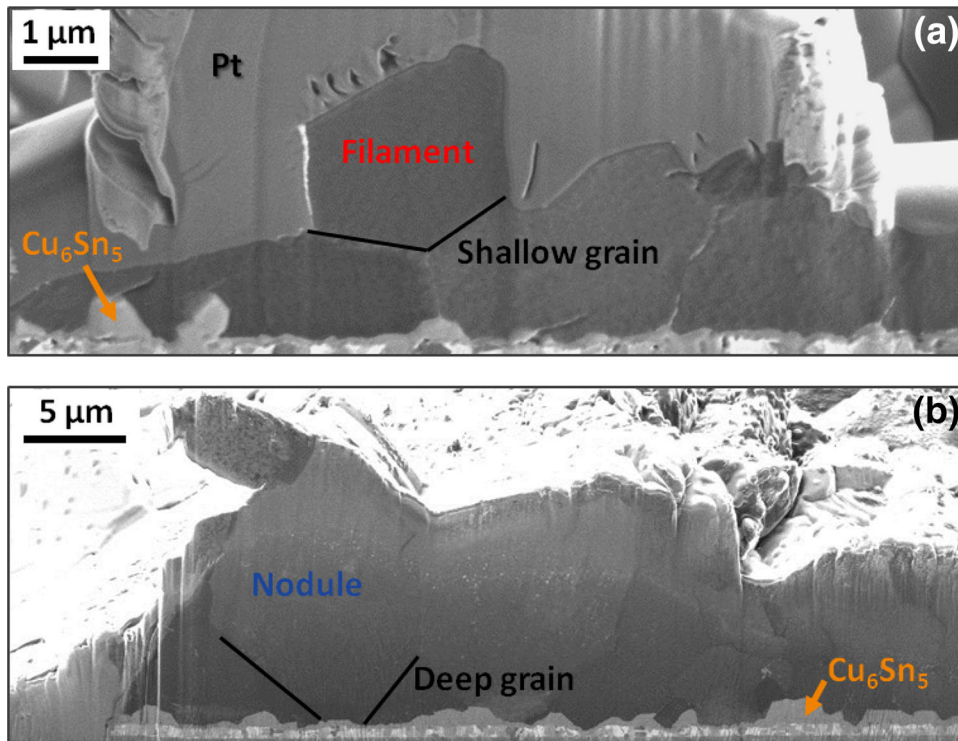


Fig. 10. Ion-channeling images of cross-sectioned matte Sn including (a) filament-type whisker for thin Sn films electroplated at current density of 25 mA/cm<sup>2</sup> stored at 30°C in dry air after 500 h, and (b) nodule for thick Sn films electroplated at current density of 25 mA/cm<sup>2</sup> stored at 30°C in dry air after 4000 h.

dislocations or newly formed Sn subgrains in the nodule; however, bending contours were observed. In addition, the nodule is a single-crystalline BCT structure with growth direction of  $[-111]$ , the same as for the filament-type whisker. The cracked surface on the deformed regions at early time was investigated to observe the microstructure of nodules at the starting point of their formation. Figure 14 presents BF TEM images and SAED patterns of thick Sn films, including a cracked surface, stored in ambient condition for 400 h. From analysis of the SAED patterns, newly formed Sn subgrains were observed in other grains; however, there were no subgrains in the grain that was assumed to be a nodule. In addition, the grain had a single-crystalline structure with  $[001]$  grain orientation. The grain causing the crack was a nodule at an early stage. In other words, cracks occur due to grain-boundary sliding with the growth of a nodule grain.

#### Growth Mechanism for Whiskers on Plastically Deformed Sn Films

In this study, matte Sn films were plastically deformed by external pressures, and were subsequently stored in ambient condition at room temperature. Thus, two environmental factors should be considered for whiskering: the external pressure and temperature. First, the external pressure is a key factor for whiskering on plastically deformed Sn

films. However, the external pressure is not the direct driving force for formation and growth of Sn whiskers because Sn whiskers were not observed in the plastically deformed regions right after the external pressure was applied. Therefore, the effect of the external pressure on Sn whisker growth is related to the recrystallization process. Because the melting point of Sn is relatively low, recrystallization can occur in Sn films even below room temperature. From the microstructure observations above, some grains grew larger than the original grains with increasing time. In addition, highly accumulated dislocations were observed in the deformed grains and at grain boundaries, and the presence of newly formed fine Sn subgrains was also confirmed. Of course, a new grain is not generated during Sn whisker growth in all cases. Chason et al. reported on a Sn whisker growth mechanism in which a new grain is not formed under thermally induced stresses.<sup>16,17</sup> In this work, however, newly formed grains were related to deformation-induced Sn whisker growth, which is similar to the study of Vianco and Rejent.<sup>18</sup> They suggested that Sn whiskers grow according to a dynamic recrystallization model, and newly formed grains are without dislocations. Therefore, it is suggested that the Sn films were recrystallized by the external pressure. In addition, the recrystallized grains affected the driving force for Sn whisker growth on the plastically deformed Sn films. Second, the effect of room

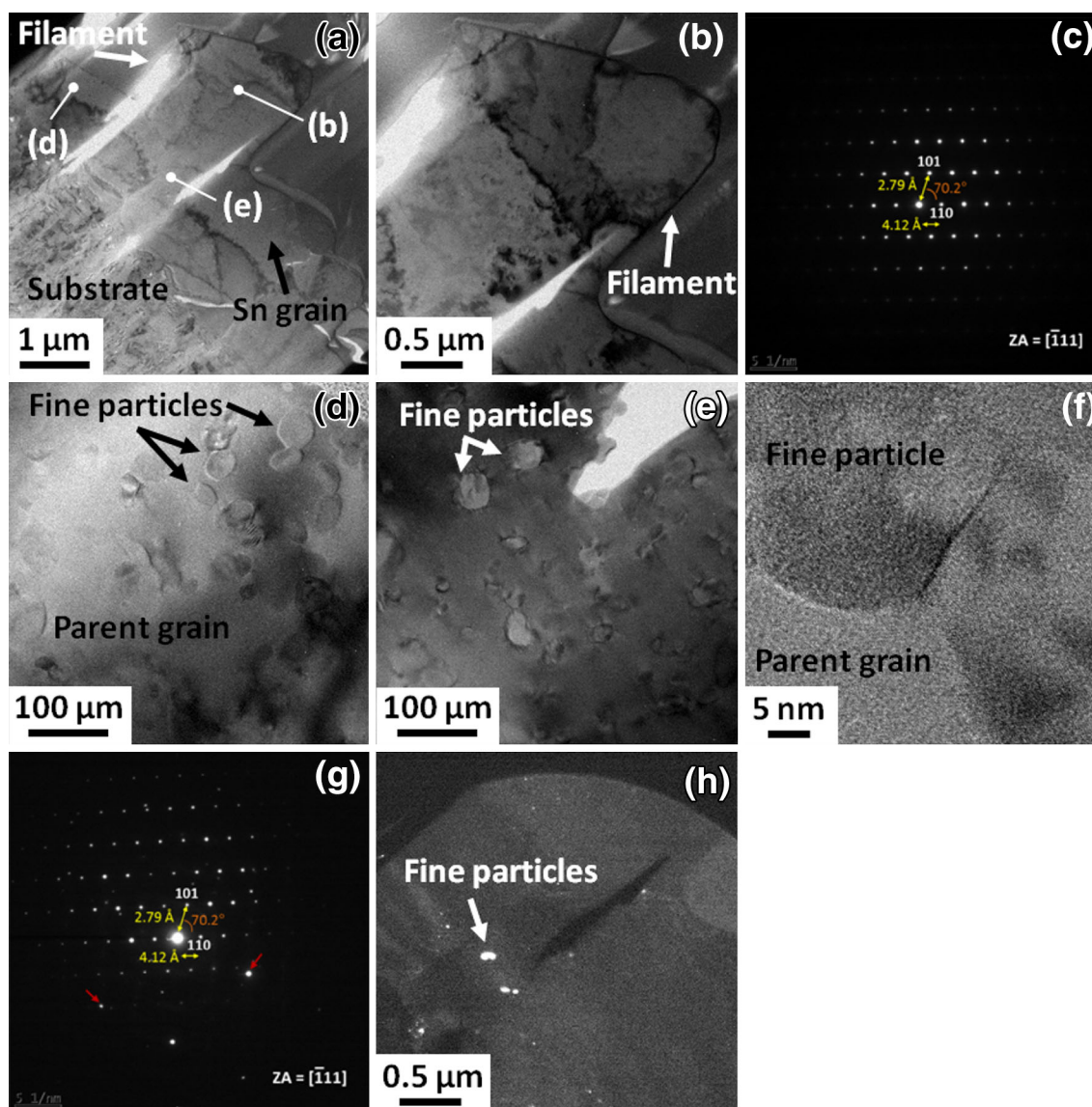


Fig. 11. TEM analysis of plastically deformed region on matte Sn stored at 30°C in dry air after 500 h: (a) BF image of deformed region including filament-type whisker and neighboring grains, (b) BF image of magnified view of a filament-type whisker, (c) SAED patterns of (b), (d) BF image of a magnified view of a grain directly contacted by external pressure, (e) BF image of a magnified view of a grain under the filament-type whisker, (f) HRTEM image of fine particle in (d), (g) SAED patterns of (e), and (h) DF image of (e).

temperature on Sn whisker growth is related to  $\text{Cu}_6\text{Sn}_5$  IMC growth.<sup>19,20</sup> When Cu atoms from the substrate diffuse into the Sn film, the increasing volume due to IMC growth at grain boundaries induces compressive stress in the Sn finish, even at room temperature. During this period, Sn oxide on the surface of the Sn film would prevent defect annihilation, leading to compressive stress build-up in the Sn films. When the surface oxide cracks, probably along a certain grain boundary, this compressive stress would be relieved by extruding the Sn grain itself, and Sn atoms diffuse into the stress-relieved grain from neighboring grains. This mechanism is the Sn whisker growth mechanism in ambient condition of room temperature.<sup>6,7,20</sup> Similarly, in this study,  $\text{Cu}_6\text{Sn}_5$  IMC was not observed at

the interface between the Sn film and Cu substrate layer for both as-plated and as-deformed Sn films, because there is not much time to form  $\text{Cu}_6\text{Sn}_5$  IMC, as shown in Fig. 3. However, growth of  $\text{Cu}_6\text{Sn}_5$  IMC was observed at room temperature after 500 h to 4000 h, as shown in the FIB cross-sections of Fig. 10. The thickness of  $\text{Cu}_6\text{Sn}_5$  was 0.7  $\mu\text{m}$  and 1.2  $\mu\text{m}$  at the interface between the Sn film and Cu layer when stored under ambient condition for 400 h and 4000 h, respectively. Therefore,  $\text{Cu}_6\text{Sn}_5$  IMC growth can also affect the whisker growth on plastically deformed Sn films.

Here, we propose a growth mechanism for Sn whiskers on plastically deformed Sn films based on two microstructural processes observed: recrystallization and  $\text{Cu}_6\text{Sn}_5$  IMC growth. Figure 15

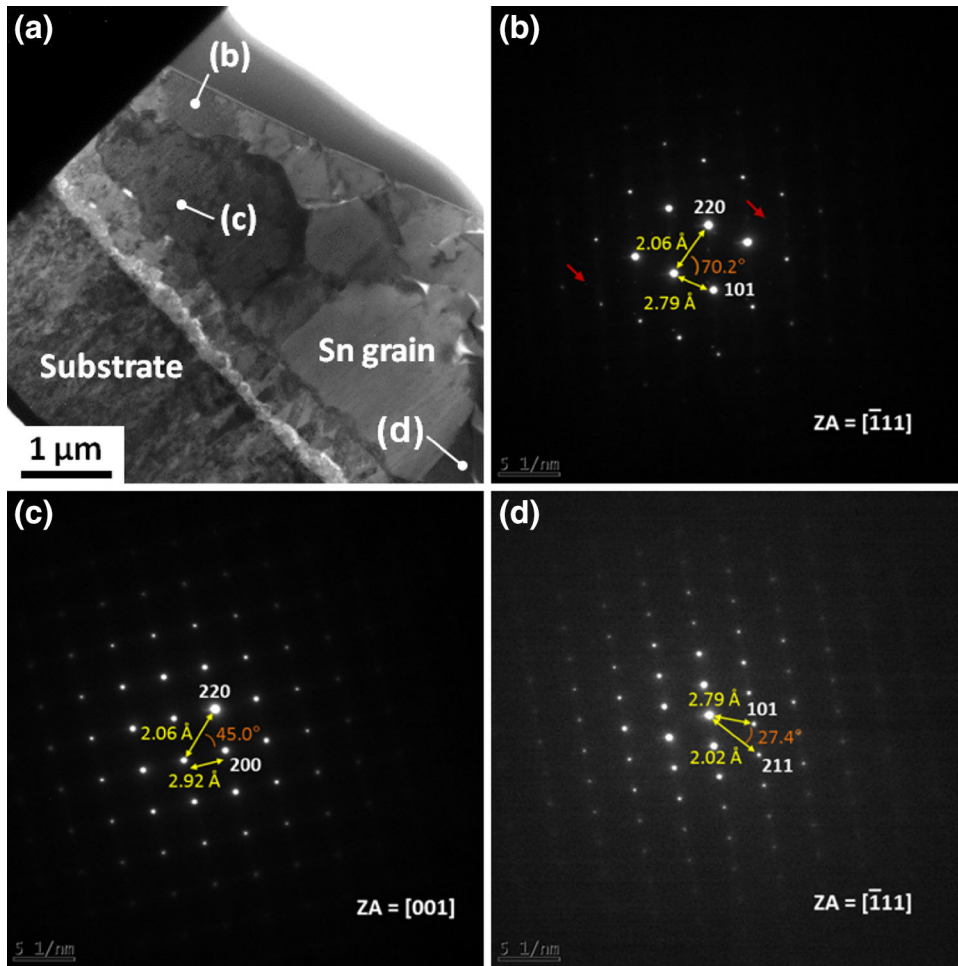


Fig. 12. TEM analysis of plastically deformed region in as-deformed matte Sn: (a) BF image, and (b–d) SAED patterns.

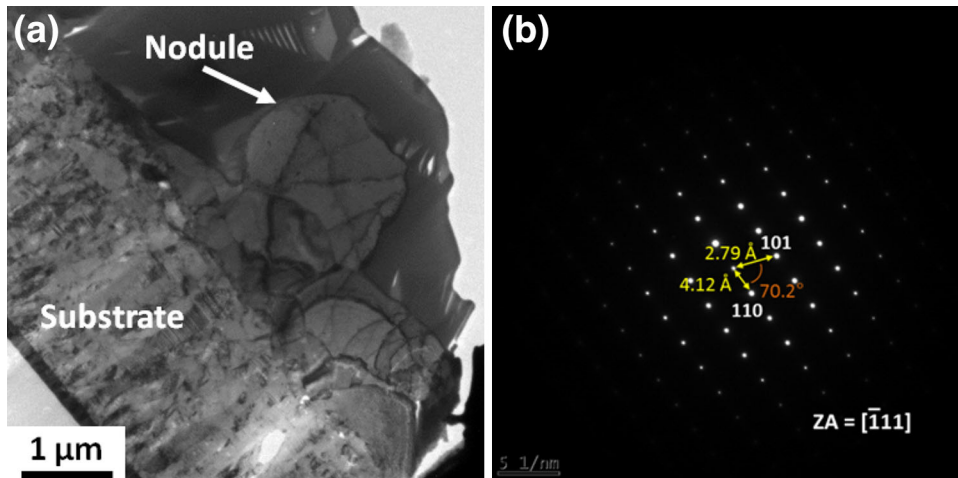


Fig. 13. TEM analysis of a fully grown nodule on plastically deformed region in matte Sn stored at 30°C in dry air after 4000 h: (a) BF image, and (b) SAED pattern.

presents schematic diagrams of the growth mechanism for deformation-induced Sn whiskers for two whisker groups, i.e., filament-type and nodule. First, filament-type whiskers are mostly observed

on thin Sn films, which have small columnar grain structures. However, the small columnar grains are inclined and horizontal grain boundaries are formed when an external pressure is applied to the

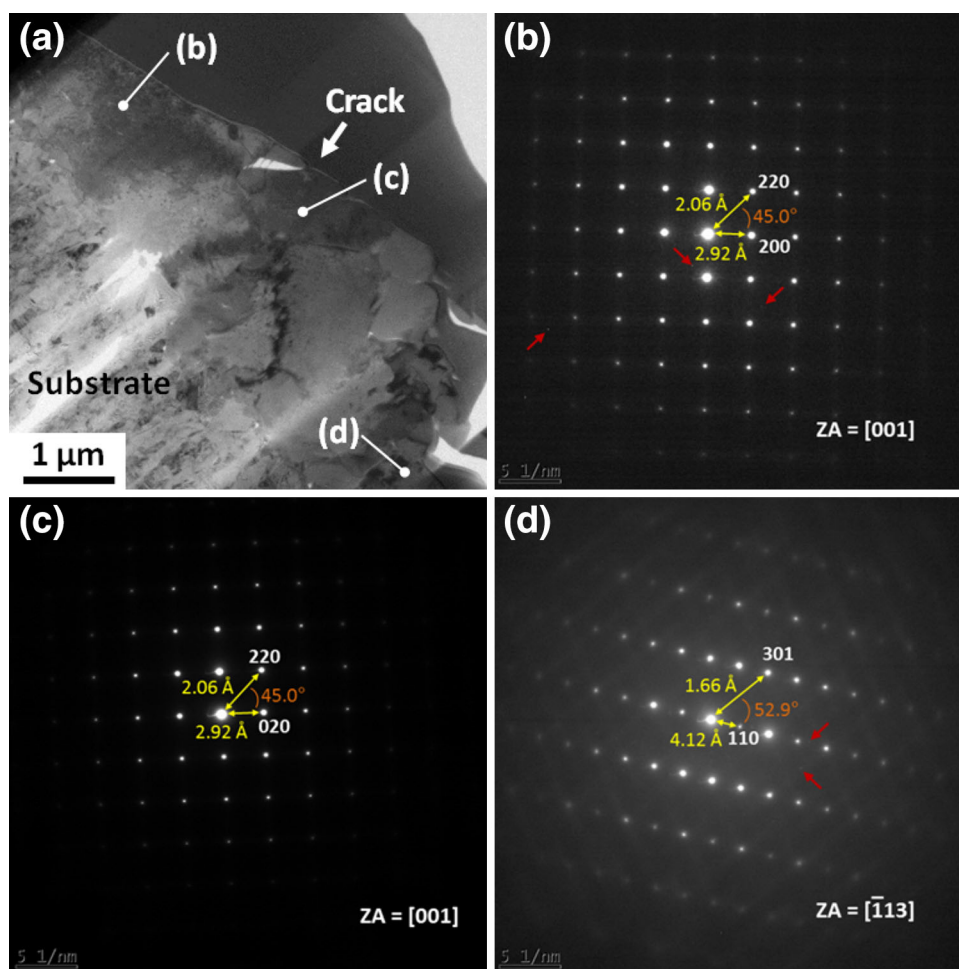


Fig. 14. TEM analysis of plastically deformed region on matte Sn stored at 30°C in dry air after 400 h, including a crack: (a) BF image, and (b–d) SAED patterns.

Sn films. In addition, the plastic deformation creates dislocation pileups at preexisting grain boundaries. Subgrains are newly formed in the grains where an external pressure is directly applied. These newly formed fine subgrains grow into the deformed Sn films by grain-boundary migration. Then, internal stresses are generated in the Sn films resulting from the recrystallized grains, which grow larger than the original grains. Next, certain recrystallized Sn grains extrude out from the Sn films as a filament-type whisker to relieve the internal stresses. Thereby, the driving force induced by the recrystallization is reduced because it is used to form Sn whiskers. However, the Sn whiskers can grow continuously to release the compressive stress induced by  $\text{Cu}_6\text{Sn}_5$  IMC growth. Namely, the formation of Sn whiskers is determined by the recrystallization resulting from the external pressure, and the growth of Sn whiskers is sustained by the  $\text{Cu}_6\text{Sn}_5$  IMC growth at room temperature. Therefore, more Sn whiskers can nucleate faster due to the recrystallization process induced by an external pressure. However,

the compressive stresses resulting from  $\text{Cu}_6\text{Sn}_5$  IMC growth are easily relieved because the small columnar grains begin to become inclined, a configuration that is effective for releasing compressive stresses. Thus, the length of deformation-induced Sn whiskers appears to be shorter than for nondeformed Sn films. The growth mechanism for a nodule is somewhat different from that of filament-type whiskers. The dislocation accumulation and formation of new subgrains resulting from external pressure are identical to those for the growth of filament-type whiskers. However, nodules are mostly observed on thick Sn films, which have large equiaxed grains. Therefore, the recrystallized grains grow continuously rather than undergoing filament formation to reduce the strain energy in the Sn film, because the neighboring grains are relatively large and the strain energy is relatively low due to the equiaxed grain structure. In addition, the recrystallized grain is limited to a size commensurate with the neighboring grain. Nevertheless, the strain energy continues to be induced by  $\text{Cu}_6\text{Sn}_5$  growth, as does the driving

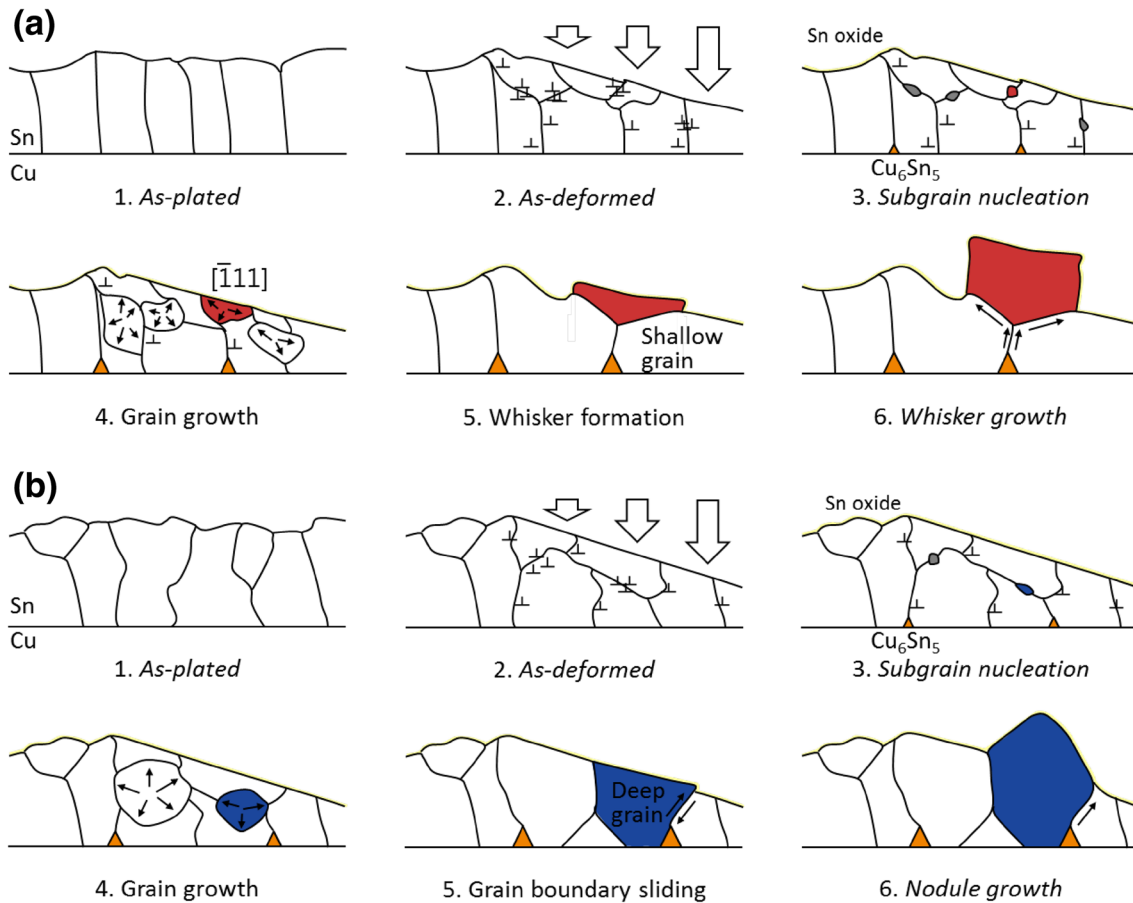


Fig. 15. Schematic diagrams of growth mechanism for deformation-induced Sn whiskers for (a) filament-type whiskers, and (b) nodules.

force to reduce the resulting strain energy. At this time, the recrystallized grain uplifts through the surface as a nodule with grain-boundary sliding.

### CONCLUSIONS

Plastically deformed matte Sn films were investigated to understand deformation-induced Sn whiskers. The effects of plastic deformation on Sn whisker growth were evaluated. In addition, the density, length, and kinetics of Sn whiskers in plastically deformed regions were examined for different plating thicknesses and current densities to determine the effect of these variables on the mitigation of deformation-induced Sn whiskers. Finally, growth mechanisms of deformation-induced Sn whiskers are proposed based on the processes of recrystallization and IMC growth. The following conclusions can be drawn from this study:

1. Sn whiskers are observed on plastically deformed regions of Sn films under ambient condition for both thin and thick Sn films, regardless of the current density applied.
2. The plastic deformation induced by an external pressure promotes whisker formation on Sn films. However, the average length of Sn

whiskers in deformed regions is shorter than for nondeformed Sn films. Thin Sn films have many more filaments than nodules.

3. Sn films are recrystallized by an external pressure. Highly accumulated dislocations and newly formed fine Sn subgrains are observed at the deformed grains and grain boundaries. In addition, recrystallized grains and  $\text{Cu}_6\text{Sn}_5$  IMC grow with increasing time.
4. The growth mechanism for deformation-induced Sn whiskers can be explained by the combined processes of recrystallization and  $\text{Cu}_6\text{Sn}_5$  IMC growth. The formation of Sn whiskers is determined by the recrystallization resulting from the external pressure, and the further growth of Sn whiskers is determined by  $\text{Cu}_6\text{Sn}_5$  IMC growth at room temperature.

Thus, we have found that control of current density and plating thickness is insufficient to suppress deformation-induced Sn whiskers on plastically deformed Sn films. However, a new Sn whisker growth mechanism is proposed to understand the behavior of deformation-induced Sn whiskers. Therefore, this study can help development of a mitigation strategy for deformation-induced Sn whisker growth in future investigation.

### ACKNOWLEDGEMENTS

This work was supported by the Global Technology Innovation Program (N02130092) funded by the Ministry of Trade, Industry, & Energy (MOTIE, Korea). The support of Tae Woo Lee of the KAIST central research instrument facility for FIB analysis is appreciated. This project was also supported by the IBM-KAIST joint study program when J.C. visited IBM T.J. Watson Research Center. The technical support of C.L. Arvin and J.D. Schuler of IBM East Fishkill is greatly acknowledged.

### REFERENCES

1. T. Shibutani, Q. Yu, M. Shiratori, and M.G. Pecht, *Microelectron. Reliab.* 48, 1033 (2008).
2. M. Osterman, Whiskers on USB housing of PC Mother Board, <http://www.calce.umd.edu/tin-whiskers/presentations/WhiskersOnUSB1-20080905.pdf>. Accessed 24 July 2014.
3. J.W. Osenbach, R.L. Shook, B.T. Vaccaro, B.D. Potteiger, A.N. Amin, K.N. Hooghan, P. Suratkar, and P. Ruengsin-sub, *IEEE Trans. Electron. Packag. Manuf.* 28, 36 (2005).
4. N. Jadhav, J. Wasserman, F. Pei, and E. Chason, *J. Electron. Mater.* 41, 588 (2012).
5. European Union, Directive 2002/96/EC of the European Parliament and of the Council of 27 January 2003 on WEEE, *Off. J. Eur. Union*, L37/24-38 (2003).
6. K.N. Tu and J.C.M. Li, *Mater. Sci. Eng. A* 409, 131 (2005).
7. W.J. Boettinger, C.E. Johnson, L.A. Bendersky, K.-W. Moon, M.E. Williams, and G.R. Stafford, *Acta Mater.* 53, 5033 (2005).
8. H. Moriuchi, Y. Tadokoro, M. Sato, T. Furusawa, and N. Suzuki, *J. Electron. Mater.* 36, 220 (2007).
9. J. Chang, S.K. Kang, J.-H. Lee, K.-S. Kim, and H.M. Lee, *J. Electron. Mater.* 43, 259 (2014).
10. A.M. Howatson, P.G. Lund, and J.D. Todd, *Engineering Tables and Data* (The Netherlands: Springer, 1972), p. 41.
11. JEDEC Standard JESD201A. Environmental Acceptance Requirements for Tin Whisker Susceptibility of Tin and Tin Alloy Surface Finishes 2008.
12. P. Sarobol, J.E. Blendell, and C.A. Handwerker, *Acta Mater.* 61, 1991 (2013).
13. F. Yang and Y. Li, *J. Appl. Phys.* 104, 113512 (2008).
14. T. Shibutani, *IEEE Trans. Electron. Packag. Manuf.* 33, 177 (2010).
15. W.F. Gale and T.C. Totemeier, *Smithells Metals Reference Book*, 8th ed. (Butlington: Elsevier, 2003), pp. 6–18.
16. E. Chason, F. Pei, C.L. Briant, H. Kesari, and A.F. Bower, *J. Electron. Mater.* 43, 4435 (2014).
17. F. Pei, C.L. Briant, H. Kesari, A.F. Bower, and E. Chason, *Scripta Mater.* 93, 16 (2014).
18. P.T. Vianco and J.A. Rejent, *J. Electron. Mater.* 38, 9 (2009).
19. K.N. Tu and R.D. Thompson, *Acta Metall.* 30, 947 (1982).
20. B.-Z. Lee and D.-N. Lee, *Acta Mater.* 46, 3701 (1998).